Assiut University Journal of Chemistry (AUJC) 44(2015) 50-64

Journal homepage: www.aujc.org

ISSN 1678-4919

Vol(44)	No(2)	2015

Full Paper

The influence of the activation conditions on the textural characteristics of the activated carbons obtained from local peanut shells

M.M. Girgis[a],B.M. Abu-Zied[a] and F.E.M. El-Darrat[b]
[a]Chemistry Department, Faculty of Science, Assiut University, Assiut
[b]Chemistry Department, Faculty of Science, 7 October University, Misurata, Libya.

E-mail address: mmgirgis2005@yahoo.com

Article history : Received: 23/2/2015 ; Revised :26/5/2015 ; Accepted :16/6/2015 ; Available Online : 24/11/2015;

Abstract:
Surface area and pore structure of activated carbons (ACs) prepared from peanut shells were estimated for seven samples of ACs variable in their activation method. Characterization of the porous structure of these ACs was evaluated by scanning electron microscopy and analysis of the respective N_2/77 K adsorption-desorption isotherms. Surface areas accessible to MB (S_{MB}) =110-813 m^2/g were calculated using the Langmuir and Freundlich adsorption isotherm equations. The Langmuir adsorption isotherm model gives better fit as compared to Freundlich model. Ratios of methylene blue surface area to nitrogen surface area ($S_{MB}/S^{\alpha}_{N_2}$) were evaluated and discussed.

Keywords: activated carbons, peanut shells, surface area, methylene blue.

1. INTRODUCTION

Activated carbons (ACs) defines a group of materials with highly developed surface area and porosity, and hence a large capacity of adsorbing chemicals from gases and liquids [1-3]. Among various kinds of porous solids, ACs have the widest application in industry, science and everyday life. They have been used successfully in food processing, in water and air purification, and in chemical, pharmaceutical, petroleum mining, nuclear, automobile, and vacuum manufacture [4]. ACs can be produced by one of two ways:
i) By carbonizing materials of vegetable origin with the addition of activating agents (such as H_3PO_4 [5,6], KOH [7,8] and $ZnCl_2$ [9,10]) which influence the course of pyrolysis [1,11] . This method is known as "chemical activation". ii) By allowing the inactive carbonized product (prepared by the usual methods of carbonization) to react with suitable gaseous substances (such as steam or CO_2).This is known as "physical activation". The carbonization and activation processes can be combined to form a one-step activation process[12]. Almost every industry uses organic dyes and pigments to color its

products. Many of these substances are inert and non-toxic at the concentrations discharged into the receiving waters. However, some are not so innocuous, and in either case, the color they impart is very undesirable to the water user. In the same context, it is worth mentioning that adsorption of dyes from solution offers a simple, rapid and versatile method which can be used for the measurement of: (i) external surface area of non-porous solids; (ii) internal specific surface of porous materials accessible to solute of a range of sizes respectively; and (iii) external specific surface of porous powders [12]. Methylene blue (MB) is a standard medium-size organic dyestuff commonly used as a model compound for adsorption of organic contaminants from aqueous solution [13, 14]. It indicates adsorption within mesopores. MB test is empirically correlate with total surface in pores greater than 15 Å diameters [15]. There are quite large number of studies regarding the preparation of ACs from agricultural wastes which include a number of nutshells and other byproducts [1,12,16-18]. In comparison, peanut shells received much less consideration as a source material for the preparation of ACs,as well as the methods used for their production [2,3,14,19-21], although considerable amounts of peanut shells are annually left behind peanuts processing industries and are mainly used up till now in primitive applications. However, no work is known to us regarding the use of phosphoric acid as an activating agent in presence of steam/nitrogen atmosphere, and preparation of high surface area carbons (≥ 1000 m2. g^{-1}) with high adsorbing power from peanut shells, although this precursor is characterized by a low ash content (2.2%), very low apparent density (0.73 $g.cm^{-3}$) and high degree of porosity (54%) [22]. Also, there is a great lack in the characterization of the obtained carbons [19, 20]. The object of the present work is to investigate the influence of the activation conditions on the textural characteristics of the ACs obtained from local peanut shells, in an attempt to find out the best and optimal conditions for preparing high quality ACs from this agricultural waste product. The study aims also to investigate the adsorptive properties of these carbons towards MB as a standard medium-size organic dyestuff.

2. EXPERIMENTAL

2.1.Preparation of Activated Carbons

Clean, dried and crushed peanut shells were used for the preparation of the AC samples. Seven samples of ACs variable in their activation method were selected. For the 1st three samples, 100 grams of peanut shells were soaked in pre-diluted phosphoric acid of various concentrations.Starting with 88 wt % H_3PO_4 (BDH), the following concentrations were obtained by dilution: 30, 50 and 70 wt%. The peanut shells mass was slightly agitated to ensure penetration of the acid throughout, and left overnight at room temperature to help appropriate wetting of the precursor. Next day the impregnated sample was admitted into the reactor which was then introduced into the tubular electric furnace. The carbonization process was carried out at 600°C under a flow of steam / N_2 atmosphere. The sample was kept at 600°C for 3 h, and then cooled under N_2 atmosphere to room temperature. The carbonized product was thoroughly washed with hot distilled water for several times until the pH of the washings attained a value of 6.5. These samples were designated as PS36, PS56 and PS76, where the letters PS indicate the chemical activation by H_3PO_4 in steam / nitrogen atmosphere and the first number following these letters denotes the H_3PO_4 concentration, whereas the second number indicates the carbonization temperature.The 4th sample (P56) was prepared by impregnation with 50 wt % H_3PO_4 and carbonization at 600°C under N_2 atmosphere, followed by washing with hot water until the pH of the washings attained a value of 6.5. The 5th (CK) sample was obtained by impregnation with KOH saturated solution

(2:1 ratio) , followed by carbonization at 600^{o}C under N_2 atmosphere , followed by washing with water until the pH of the washings attained 6.5.The sixth sample (S900) was prepared by one- step steam/N_2 activation at 900^{o}C for 3 h. The last sample (C33) was obtained by two- step CO_2 activation: First, non-activated carbon (C500) was prepared by the destructive distillation of peanut shells at 500°C under a flow of N_2 (100 ml min^{-1}). The heating rate was 10°C/min. The sample was kept at 500°C for 3 hours. For the preparation of the C33 sample, 50 grams of the C500 sample were placed in the hot zone of the reactor over a stainless steel network and covered with another one. Carbon dioxide was supplied from a gas cylinder and its flow rate was controlled by a CO_2 adaptor. The rate was 2000 cm^3.min^{-1}. The sample was prepared by gasification at 700°C with CO_2, then cooled in atmosphere of CO_2 till room temperature and weight determined. The proper time for activation was adjusted to obtain 33 % burn-off level, equation (1):

Burn-off (%) = [1 - (weight of the activated carbon / weight of char)] x 100 **(1)**

The sample was designated as C33, where the number following the letter indicates the percentage burn-off.

2.2. Characterization of activated carbons

2.2. a.Scanning Electron Microscope (SEM) Investigations

For a visual inspection of external porosity and micro-texture, scanning electron micrographs of selected dried carbon samples prepared under different activation conditions were obtained using a JEOL scanning microscope, model JSM-5400 LV (Joel, Tokyo, Japan). The samples were prepared by the gold sputtering technique [23].

2.2. b.Nitrogen Adsorption

To evaluate the structural parameters of the ACs under investigation, the adsorption / desorption isotherms of nitrogen at 77 K were constructed using NOVA 3000 Multi-Station High Speed Gas Sorption Analyzer (Quanta-Chrome Corporation), Version 6.07. The adsorption isotherms were analyzed to get various porous parameters: i) The BET-equation [24] parameters: S_{BET} (BET-surface area, m^2/g), C_{BET} (the constant C of the BET equation) and $V_{P(total)}$ (total pore volume, cc/g), and ii) The α_S-plot [25] parameters: S_t^{α} (total surface area, m^2/g) , S_n^{α} (non-microporous surface area, m^2/g) , S_{mic}^{α} (microporous surface area, m^2/g), V_o^{α} (micropore volume, cc/g), $\bar{r}$ (mean pore radius, Å) and V_{meso} (mesopore volume, cc/g).

2.3. Adsorption of Methylene Blue

2.3.a. Technique

A stock aqueous solution (1000 ppm) of MB was prepared. Other solutions of MB were prepared from this solution by dilution to the required concentration. For adsorption experiments, 50 mg of the powdered carbon sample, which was dried in an oven at 110°C for 2 h, was weighed in different stopper Pyrex bottles of 100 ml capacity and 50 ml of dye solutions of known concentration were added in increasing amounts. The bottles were then fixed in a shaker placed in an air thermostat maintained at 25°±0.2°C. The shaker was subjected to a rotary motion about 120 revolutions per minute. The bottles with their contents were shaken for 72 h for equilibrium. Preliminary experiments proved that a period of 48 h was sufficient to attain equilibrium conditions. The supernatant liquid was removed and analyzed spectrophotometrically using a double beam computerized UV/Visible Scanning Spectrophotometer [type Shimadzu (UV-2101 PC)] and a1cm length-path cell. The wavelength was selected so as to obtain maximum absorbance for MB; the λ_{max} value is 662.5 nm. In accordance with the Lambert-Beer's law the absorbance was found to vary linearly with concentration and dilutions were undertaken when the absorbance exceeded 0.7. The amount adsorbed was computed from the difference between the initial and the equilibrium concentrations of

MB in the aqueous solution [6].

2.3. b.Analysis

Surface areas accessible to MB were calculated using the Langmuir and Freundlich adsorption isotherm equations:

1- The Langmuir equation is given in the linear form:

$$\frac{C_{eq}}{X} = \frac{1}{K_L X_m} + \frac{1}{X_m}.C_{eq} \qquad \textbf{(2)},$$

where C_{eq} = dye concentration in bulk solution at equilibrium (mg/l); X = the amount adsorbed at equilibrium per unit weight (mg/g); X_m= the amount adsorbed to form a monolayer (mg/g); and K_L= an empirical constant related to the energy of adsorption. X_m and K_L are indicators of limiting adsorption capacity and free energy, respectively.

2- The linear form of the Freundlich equation appears as:

$$Log\ X = Log\ K_F + \frac{1}{n} Log\ C_{eq} \qquad \textbf{(3)},$$

where K_F and n are characteristic constants. They are indicators of adsorption capacity and intensity, respectively: n > 1, is generally associated with high affinity of the adsorbent towards the adsorbate, and an increase in K_F indicates higher adsorption capacity[26]. In the application of equations (2 and 3) linear regression analysis was employed using the least-squares method. The correlation coefficient (r) was evaluated so as to determine the linearity and dispersion of points around the straight line. From the slope and intercept, in each case, the isotherm parameters were calculated.

3. RESULTS AND DISCUSSION

3.1. Scanning Electron Microscope (SEM) Observations

The evolution of the porosity after pretreatment and/or activation was studied at a macroscopic scale by scanning electron microscopy. The results are shown in Fig.(1(a-e)). Careful examination of the SEM pictures shows that the morphology of the particles depends strongly on the sample mode of activation as follows:

1- Fig. (1(a)) shows that the grains of the PS76 sample exhibit large degasification pores in a carbonaceous matrix. The surface is very rough and present a high density of pores of different sizes and shapes with diameters varying from 140 to 310 Å. The grains exhibit a sponge-like structure.

2- To illustrate the effect of the nature of the activating agent (H_3PO_4 or KOH) on the external surface appearance and micro texture of the carbon formed, the surfaces of the P56 and CK samples were examined, c.f. Fig.(1(b and c)). After H_3PO_4-pretreatment and pyrolysis at 600°C in N_2 atmosphere, the grains surface is quite rough and presents a high density of holes with different shapes and sizes. The particles exhibit large degasification pores in a carbonaceous matrix and reflect the vegetable origin, c.f. Fig.(1(b)).On the other hand, after KOH-pretreatment under the same conditions , i.e. pyrolysis at 600°C in N_2 atmosphere, the peanut shells gave a carbon consists of fine grains. The CK-sample possesses surfaces exhibit microporosity and reflects a high density of holes with diameters varying from 15 to 40 Å, c.f. Fig. (1(c)).

3- To examine the effect of the activating atmosphere (steam or CO_2) on the morphology and porosity of the carbons obtained by physical activation of peanut shells, the S900 and C33 samples were investigated. As can be inferred from Fig. (1(d)), when peanut shells were carbonized in steam at 900°C, an extensive development of porosity was observed. The S900 particles exhibit large degasification pores. The grains preserved some of the botanical arrangement. The carbonaceous material featuring a sponge-like structure. The holes diameters varying between 130 and 250 Å. Group of white particles, filaments and spheres can clearly be observed in some holes in the micrographs, which could be associated with coalesced ash or sintered particles. On the other hand, when peanut shells were carbonized in CO_2 gas to 33 % burn-off

value, the carbonaceous material produced shows rough surfaces which present a very high density of holes, c.f. Fig. (1(e)). With higher magnification (x7500), microspores with varying diameters in the range 3-8 Å can be observed. Groups of white spheres can clearly be observed which could be,also, associated with coalesced ash or sintered particles.

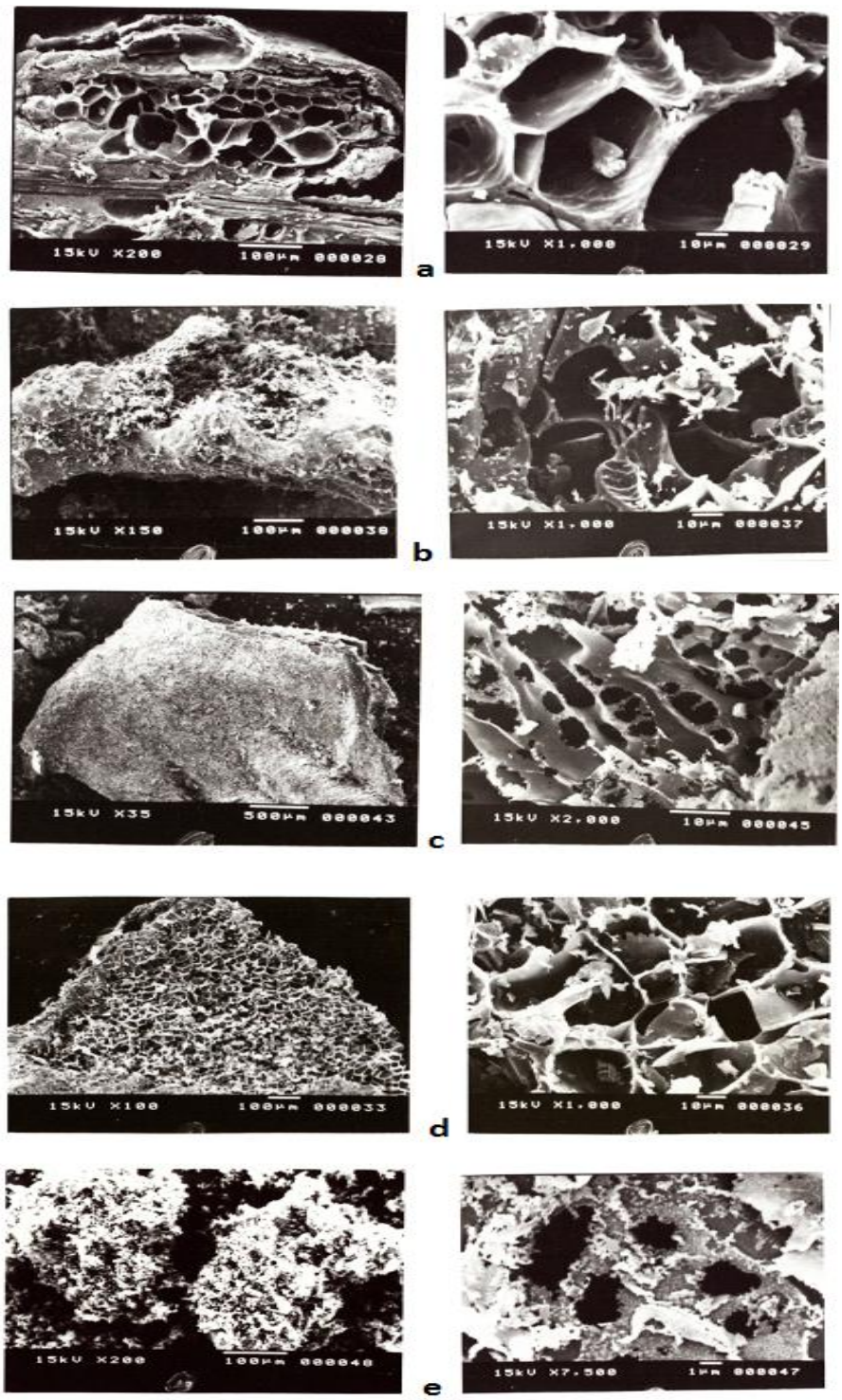

Fig.1. SEM micrographs of the external structure of the PS76 (a), P56 (b), CK (c), S900 (d), and C33 (e) samples at different magnifications.

3.2.Porosity characteristics of activated carbons

The sorption isotherms of N_2 at 77 K for the AC samples exhibit type I feature in the BDDT classification[27] with sharp "knee" at the low pressures end and very little of the type IV features at relative higher pressures. This indicates a developed microporosity with some mesoporosity and capillary condensation[28]. The sorption isotherms for the PS36, PS56 and PS76 samples are given in Fig.(2), their corresponding BET-plots are represented in Fig.(3), whereas their α_S -plots are shown in Fig.(4). The α_S– plots complement the observation obtained from the sorption isotherms of developed carbon microporosity with some mesoporosity, as these plots exhibit features of the α-2 type of the α_S -plots classification [29] for all samples. The evaluated texture characteristics obtained from the BET-equation and α_S -plots are summarized in Table (1).

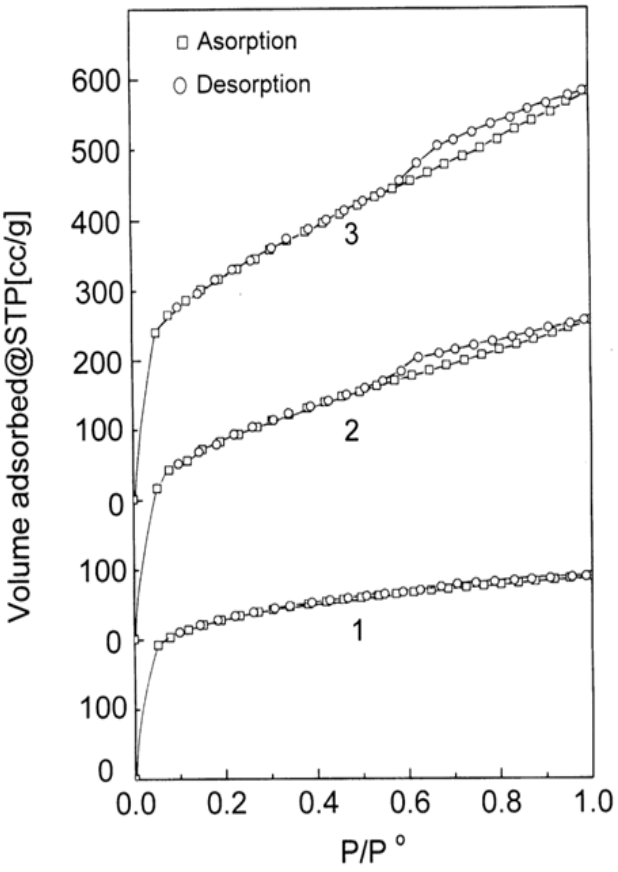

Fig. 2. Nitrogen sorption isotherms at 77K for the H_3PO_4 – activated carbons heat treated at 600°C in steam/nitrogen atmosphere: 1) 30wt% , 2) 50wt% , and 3) 70 wt% H_3PO_4.

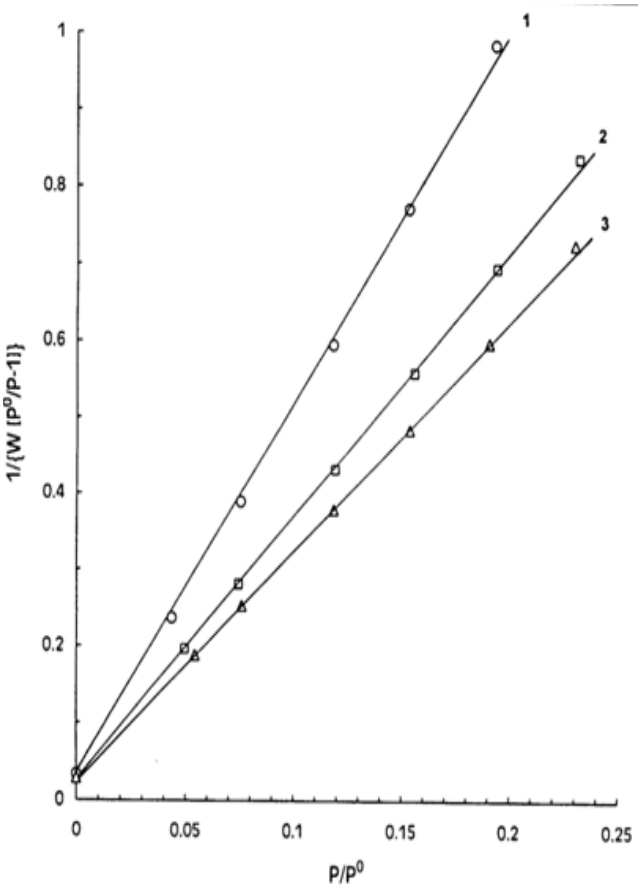

Fig.3. BET-Plots of H_3PO_4- activated carbons heat treated at 600°C insteam/nitrogen atmosphere:1) 30wt% , 2) 50 wt %, and 3) 70 wt % H_3PO_4.

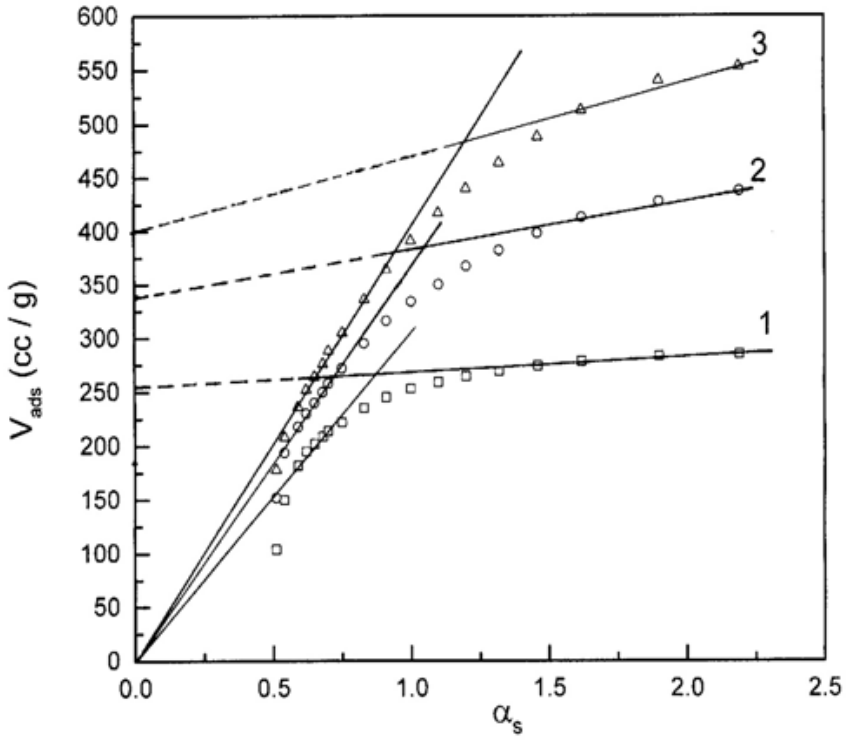

Fig. 4. α_s-Plots of H_3PO_4- activated carbons heat treated at 600°C in steam/nitrogen atmosphere: 1) 30 wt % , 2) 50 wt % ,and 3) 70wt % H_3PO_4.

Table 1: Porous characteristics of the ACs obtained from peanut shells under different activation conditions.

Sample notation	S_{BET} (m^2/g)	C_{BET}	$V_{P(total)}$ (cc/g)	α_S– plots						$S^{\alpha}_{mic}/S^{\alpha}_{t}$ (%)	$S^{\alpha}_{n}/S^{\alpha}_{t}$ (%)	$V_{mic}/V_{p(total)}$ (%)	$V_{meso}/V_{p(total)}$ (%)
				S^{α}_{t} (m^2/g)	S^{α}_{n} (m^2/g)	S^{α}_{mic} (m^2/g)	V^{α}_{0} (cc/g)	$\bar{r}$ (Å)	V_{meso} (ee/g)				
PS36	847	202	0.447	888	33	855	0.399	10.1	0.048	96.3	3.7	89.3	10.7
PS56	1026	209	0.705	1049	193	856	0.525	13.4	0.180	81.6	18.4	74.5	25.5
PS76	1154	144	0.899	1156	194	962	0.619	15.6	0.280	83.2	16.8	68.9	31.1
P56	930	403	0.610	986	90	896	0.483	12.4	0.127	90.9	9.1	79.2	20.8
CK	260	184	0.162	270	16	254	0.139	12.0	0.023	94.1	5.9	85.8	14.2
S900	334	151	0.169	342	12	330	0.152	9.9	0.017	96.5	3.5	89.9	10.1
C500	15	54	0.014	16	9	7	0.004	17.5	0.010	43.7	56.3	28.6	71.4
C33	511	383	0.217	627	12	615	0.202	6.9	0.015	98.1	1.9	93.1	6.9

A comparative representation of the data for total surface area (S_t^{α}), microspore surface area (S_{mic}^{α}) and non-microporous surface area (S_n^{α}) obtained from the α_S-plots for the samples under consideration are given in Fig. (5). The following can be observed : 1) Comparing the texture parameters of the PS36, PS56 and PS76 samples , it appears that the increase in the amount of H_3PO_4 used in the activation is accompanied by an appreciable development in these parameters. 2) Comparing the evaluated texture parameters of the P56 sample with those of the corresponding PS56 sample reflects that an AC with more developed porosity is obtained in steam / nitrogen atmosphere rather than in nitrogen atmosphere. 3) The KOH-treated carbon (CK) reflects a well-developed porous material containing a wide spectrum of pores essentially microspores with ultramicropores, supermicropores and mesopores. It appears from Table (1) that a relatively low grade AC is produced under the prescribed activation conditions. 4) Physical activation of peanut shells in steam / nitrogen atmosphere at 900°C produces microporous carbons with wide microporosity (C900). 5) The texture characteristics of the non-activated (C500) and CO_2-activated carbon (C33) samples indicate the following: a) the non-microporous surface area (S_n^{α}) is more than 56% of the total surface area (S_t^{α}) for the non-activated C-500 sample. This percentage decreases sharply from 56.3 to 1.9% by raising the burn-off value to 33 %. b) The mesopore volume is more than 71% of the total pore volume for the C500 sample. This percentage decreases sharply to 6.9% by raising the burn-off value to 33 %. Hence, the CO_2-activated sample possesses essentially microporous character. Activation to 33 % burn-off opens and widens microporosity with a slight shift to meso- and macroporosity.

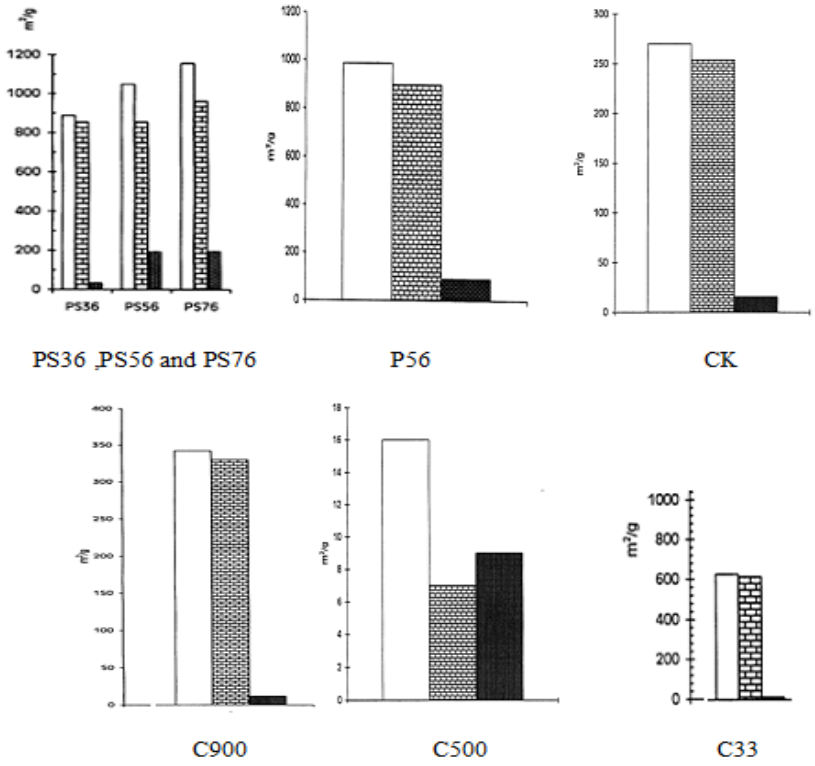

Fig.5. A comparative representation of the data for total surface area ( ); microspore surface area ( ); and non- micro porous surface area ( ); obtained from the α_S– plots for the different activated carbons.

3.3.Adsorption of Methylene Blue

Fig. (6) shows the adsorption isotherms of MB on the H_3PO_4-activated carbons heat treated at 600°C in steam/nitrogen atmosphere. The graphs are plotted in the form of amount of MB adsorbed (X) per unit mass of carbon, against the concentration of MB remaining in solution, C_{eq}. The adsorption isotherms show type-H according to the Giles classification [30]. They show very steep behavior with various degrees of sharpness or roundness at the low concentration values, tending to a plateau parallel to the C_{eq}-axis. Type-H indicates high affinity isotherm with strong preferential adsorption of the solute [30].

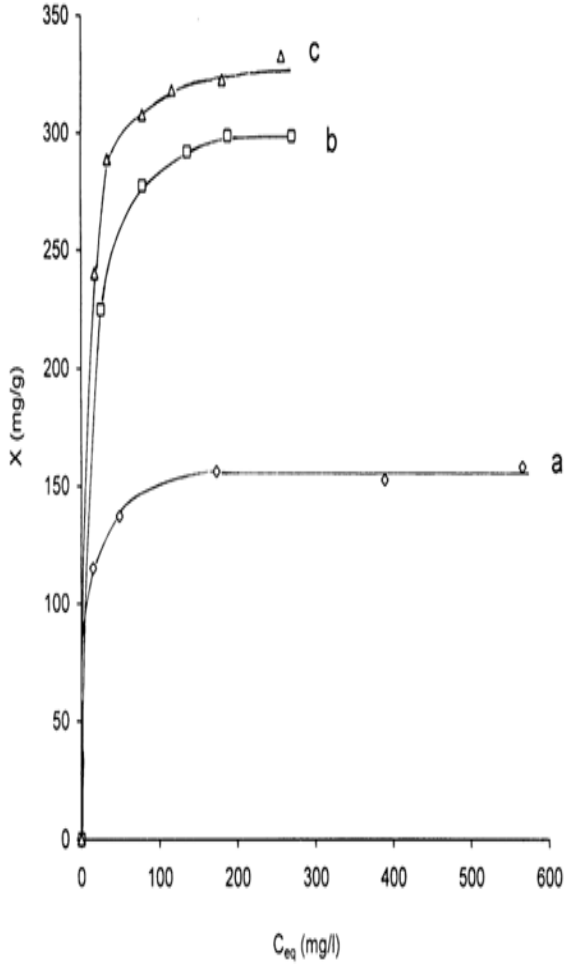

Fig. 6. Representative adsorption isotherms of MB by H_3PO_4- activated carbons obtained at 600°C in steam/nitrogen atmosphere:1) 30 wt% , 2) 50 wt %, and 3) 70 wt % H_3PO_4.

The results of the Langmuir and Freundlich plots show satisfactory straight lines, which indicate clearly that both of these adsorption models are applicable. The Langmuir plots are represented in Fig. (7), whereas the Freundlich plots are illustrated in Fig. (8).Table (2) summarizes the adsorption parameters (X_m, K_L,n_F and K_F) derived from both adsorption models. The following can be observed: i) Application of the Langmuir equation is more satisfactory as evident from their higher correlation coefficients (r) compared to those of the Freundlich equation. ii) The dye adsorption capacity increases with the increase of the impregnate concentration, the highest value is observed for the 70wt% H_3PO_4-activated carbon, i.e. the PS76 sample.

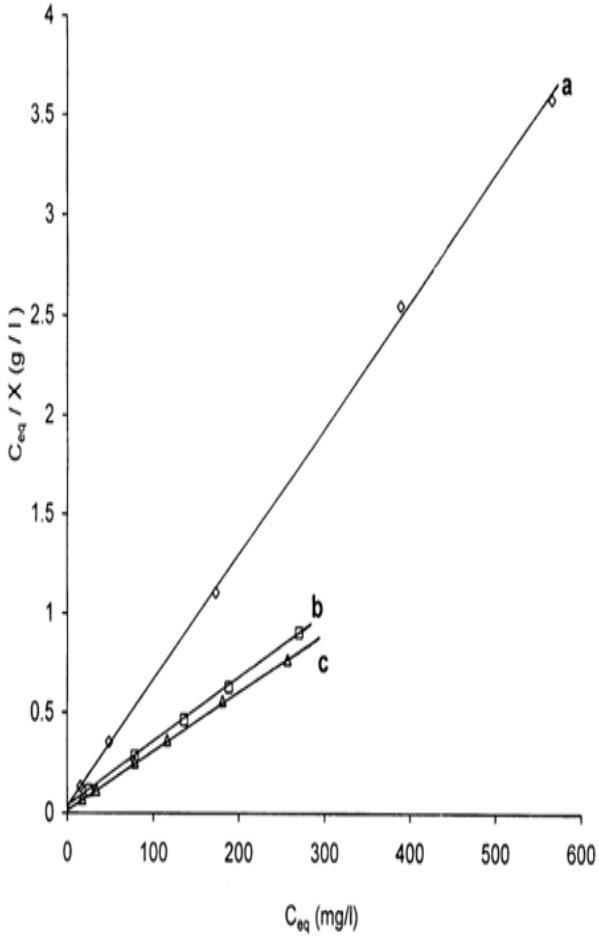

Fig.7. Langmuir plots of MB on H_3PO_4- activated carbons obtained at 600°C in steam/nitrogen atmosphere.H_3PO_4-concentration:(a) 30 wt % ,(b) 50 wt % , and (c) 70 wt %.

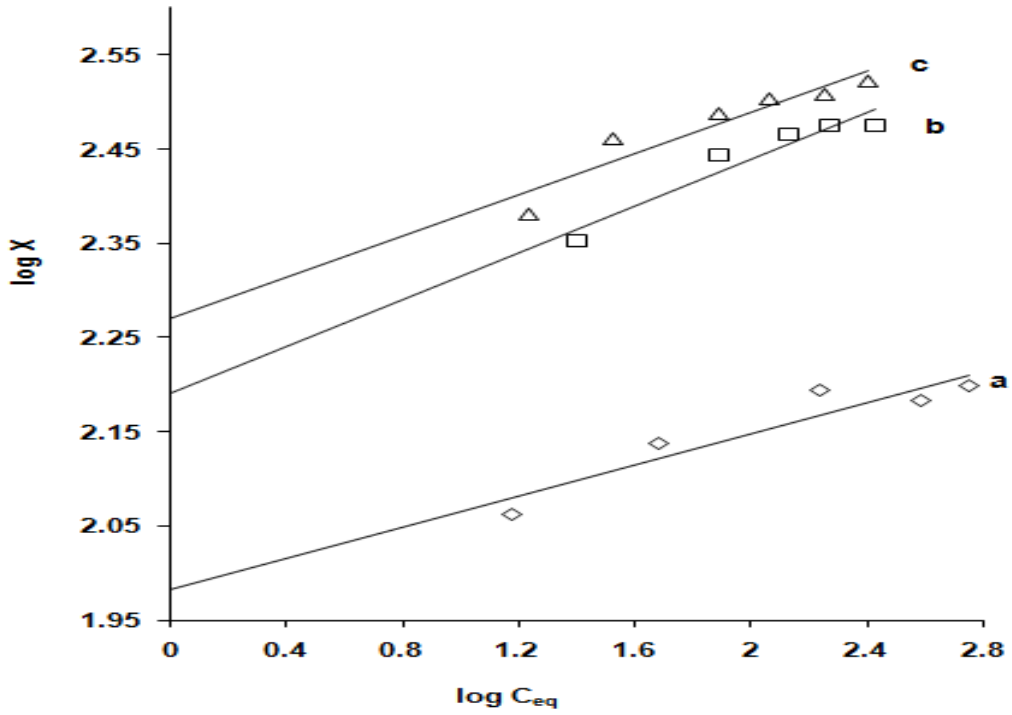

Fig.8. Freundlich plots of MB on H_3PO_4- activated carbons obtained at 600°C in steam/nitrogen atmosphere.H_3PO_4-concentration:(a) 30 wt % ,(b) 50 wt % , and (c) 70 wt %.

Table 2: Equilibrium values of methylene blue adsorption by the various activated carbons.

Sample No.	Sample notation	Langmuir-plots			Freundlich-plots		
		X_m (mg/g) at 298 k	K_L (l/mg)	r	K_F (mg/g)	n_F	r
1	PS 36	158	0.155	0.999	96	12.1	0.938
2	PS 56	310	0.113	0.999	155	8.1	0.959
3	PS 76	340	0.136	0.999	186	9.2	0.940
4	P 56	238	0.740	0.999	165	14.3	0.958
5	CK	46	0.139	0.999	29	12.3	0.996
6	S 900	66.8	0.279	0.999	40	10.7	0.856
7	C 500	14.5	0.200	0.999	5	4.6	0.979
8	C 33	120.8	0.000	0.999	105	31.9	0.893

Taking the evaluated X_m and the value of cross-sectional area covered by an adsorbed MB molecule as 120 $Å^2$ [31, 32], estimated surface areas accessible to MB (S_{MB}) are obtained (Table (3)). A comparative representation of the data for total surface area (S_t^{α}) obtained from N_2sorption isotherms and surface area accessible to methylene blue (S_{MB}) for the different activated carbons are given in Fig. (9). The results reflect an increase in the MB-accessible surface area ratio (i.e. $S_{MB} / S_{N_2}^{\alpha}$) with the increase in H_3PO_4-concentration from 30 up to 70 wt% at 600°C, c.f.Table (3) and Fig. (10).

Table 3: Surface area accessible to methylene blue and ratio to nitrogen surface area for the investigated carbons.

Sample No.	Sample notation	S_{MB} (m^2/g)	$S_{MB} / S^{\alpha}_{N_2}$
1	PS 36	378	0.426
2	PS 56	741	0.706
3	PS 76	813	0.703
4	P 56	569	0.577
5	CK	110	0.407
6	S 900	160	0.468
7	C 500	35 (17.5)*	2.188 (1.094)*
8	C 33	289	0.461

* An aggregate number of MB n = 2.

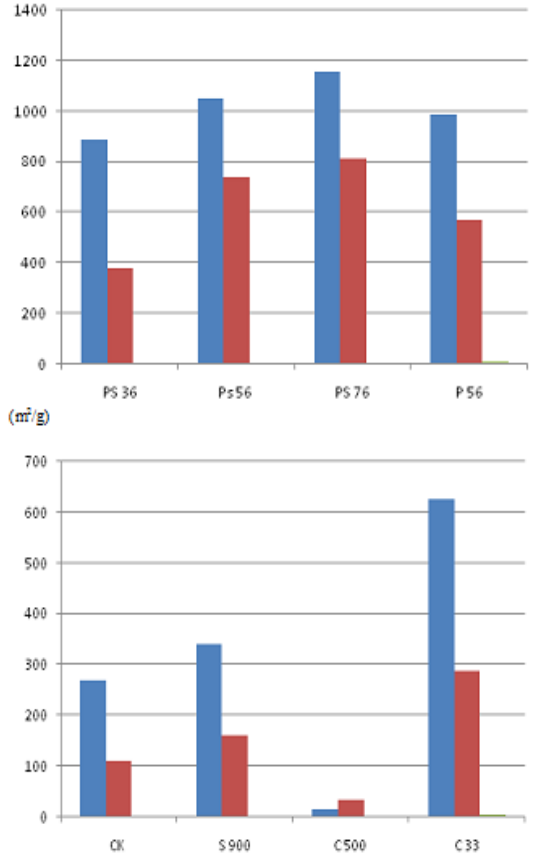

Fig . 9 . A comparative representation of the data for total surface area , S^{α}_{t} (■) obtained from N_2 sorption isotherms and surface area accessible to methylene blue, S_{MB} (■) for the different activated carbons.

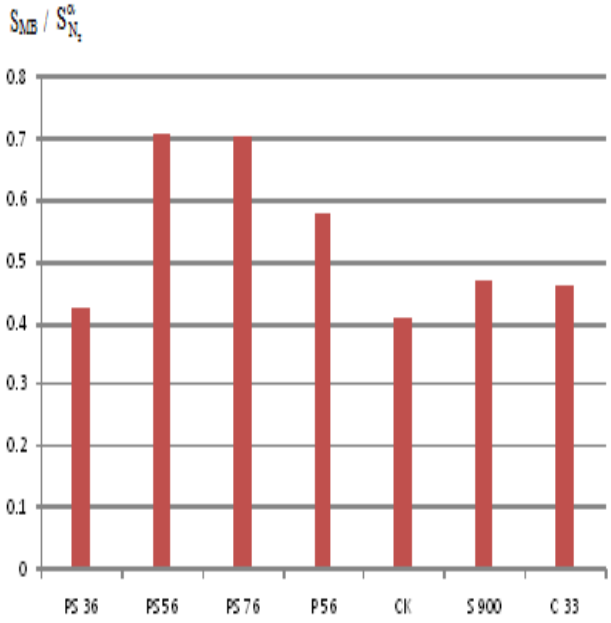

Fig .10. Ratios of methylene blue surface area to nitrogen surface area.

The adsorption isotherm of MB on the P56 sample represents typical type-H according to the Giles classification[30]tending to a plateau parallel to the C_{eq}-axis. The Langmuir parameters (X_m and K_L) and Freundlich constants (K_F and n_F) are given in Table (2). By comparing the results obtained for the PS56 and P56 carbon samples, it can be observed that the H_3PO_4-activated sample

heat treated in steam / nitrogen atmosphere (i.e. the PS56 sample) exhibit more higher affinity towards MB adsorption compared to the sample obtained under the same conditions but in nitrogen atmosphere (i.e. the P56 sample).Comparison to the nitrogen surface areas ($S^{\alpha}_{N_2}$) indicates that MB covers 0.703 and 0.577 of the nitrogen surface area for the PS56 and P56 samples, respectively, i.e. the PS56 sample shows a higher affinity towards MB adsorption. The effect of steam on the activation with phosphoric acid was found to produce carbons with more developed porosity, as indicated previously from the calculated values of S^{α}_{t} (1049 and 986 m^2/g), S^{α}_{n} (193 and 90 m^2/g) and V_{meso} (0.180 and 0.127 cc/g) for the PS56 and P56 samples, respectively. Also, the non-microporous surface area is 18.4% of the total surface area for the PS56 sample, whereas it is less than half this value (9.1%) for the P56 sample, c.f. Table (1). It should be remembered here that MB, due to its bulky size, measures only the surface area within pores of diameter ≥ 15 Å [18]. The adsorption isotherm of MB on the CK sample is represented in Fig. (11). This isotherm is analogous to the type (I) of the BDDT classification [27] and represents type-L according to the Giles classification [30]. The Langmuir and Freundlich adsorption models are applicable and show satisfactory straight lines covering the concentration range under consideration. The Langmuir and Freundlich plots are shown in Figures (12 and 13), whereas their corresponding constant parameters are given in Table (2). The estimated surface area accessible to MB molecule (S_{MB}) is given in Table (3) along with the ($S_{MB} / S^{\alpha}_{N_2}$) ratio. Comparison to the H_3PO_4-activated carbon obtained at 600°C in N_2 atmosphere (i.e. the P56 sample) indicates that MB adsorption is very much higher when the AC is produced by chemical activation with H_3PO_4 (238 $mg.g^{-1}$) rather than with KOH (46 mg/g^{-1}),Table (2). Also, MB covers a lower portion (0.407) of nitrogen surface area for KOH-activated carbon, compared to the higher one (0.577) for H_3PO_4-activated carbon. In general it can be stated that the H_3PO_4-activated carbons are characterized by very high efficiency to adsorb MB (158-340 $mg.g^{-1}$) compared to the KOH-activated carbon (46 $mg.g^{-1}$) prepared under the same conditions.

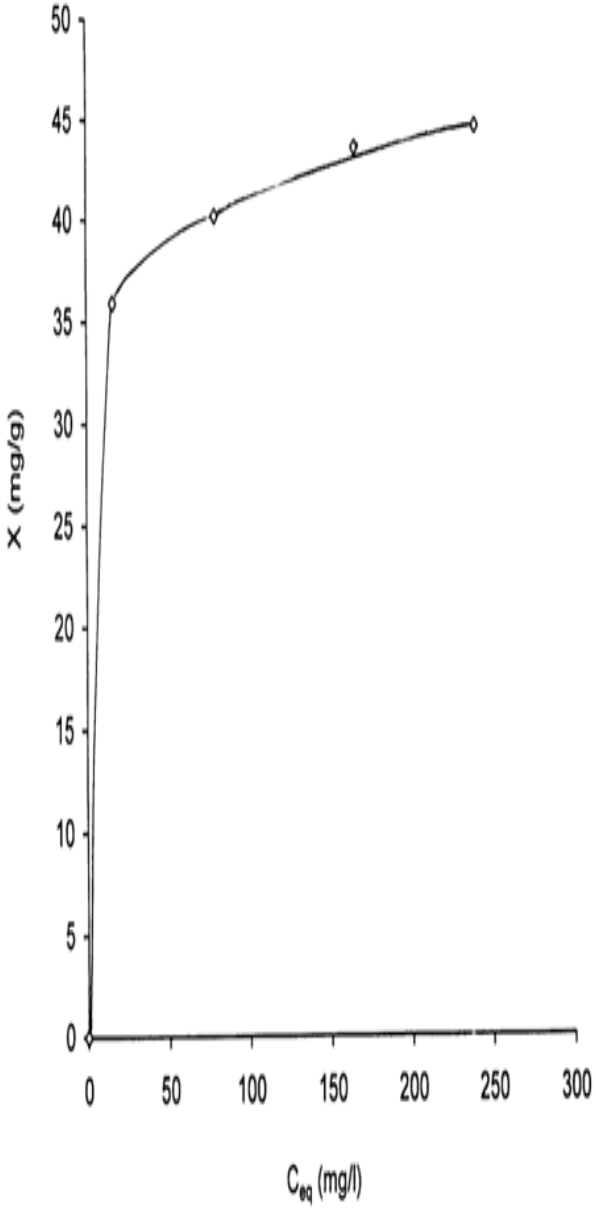

Fig. 11. Representative adsorption isotherm of MB by KOH-activated carbon.

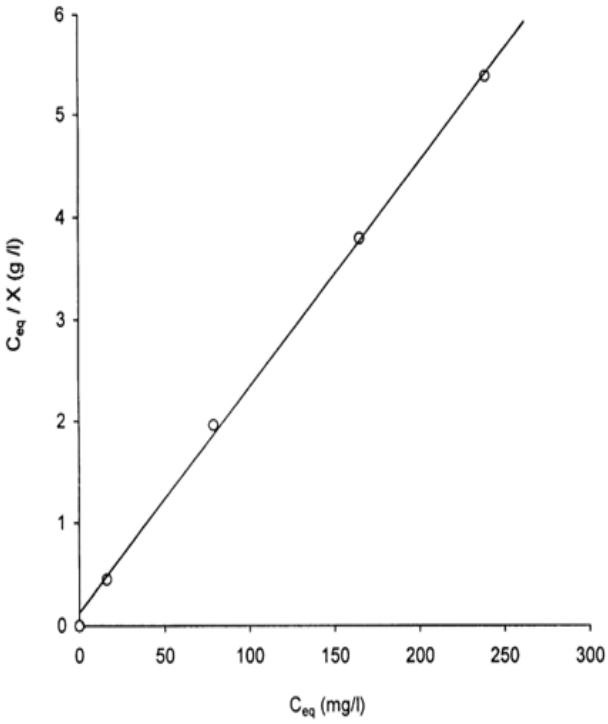

Fig.12. Langmuir plot of MB adsorption on the KOH- activated carbon.

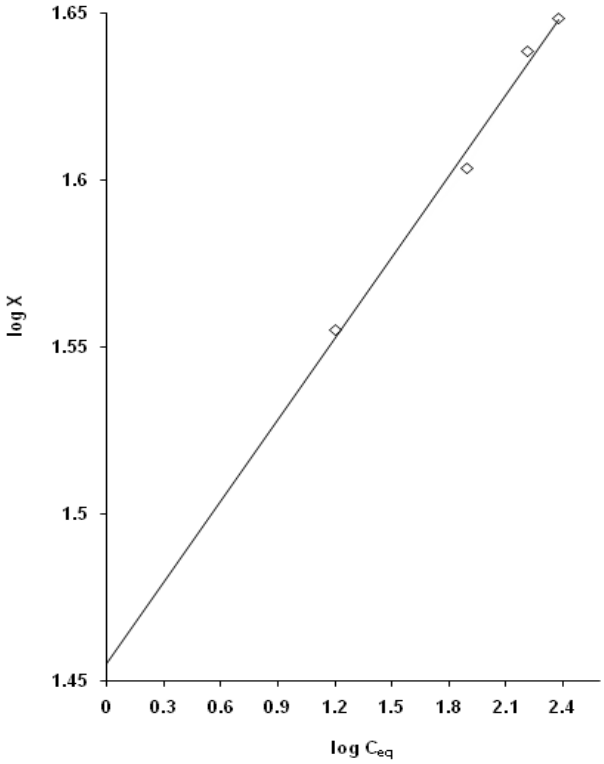

Fig.13. Freundlich plot of MB adsorption on the KOH- activated carbon.

The isotherm for the adsorption of MB on the steam-activated carbon heat treated at 900°C shows, also, type-L (the Langmuir type) according to the Giles classification [30], with very steep behavior at low concentrations and tending to a plateau parallel to the C_{eq}-axis. The obtained constants of the Langmuir and Freundlich plots are summarized in Tables (2 and 3). The relatively high adsorption of MB by the S900 sample (66.8 $mg.g^{-1}$) can be ascribed to the increased adsorption space on the carbon surface, due to the increase in the number of pores accessible to MB molecules. It can be noticed from Table (3) that MB covers a high portion (0.468) of the nitrogen surface area. The adsorption isotherm of MB on the non-activated carbon (i.e. the C500 sample) shows typical type-L according to Giles classification[30].By rising the burn-off value from 0.0 for the C500 sample to 33.0 % for the C33 sample , the adsorption isotherm changes to type-H of the same classification.

The results for the C500 and C33 samples indicate that both of the Langmuir and Freundlich adsorption models are applicable. Table (2) summarizes the obtained Langmuir and Freundlich equation constants. It can be observed a large increase in MB adsorption capacity with raising the burn-off value from 0.0% (14.5 $mg.g^{-1}$) to 33% (120.8 $mg.g^{-1}$). This can be explained by the increase in the carbon surface area as well as the MB-accessible surface area ratio (S_{MB} /S_N^{α}), as shown in Table (3). The non-activated carbon (C500) seems to adsorb much amount of MB that appears to measure much higher surface area. However, this trend may be explained if MB is imagined to be adsorbed in a compact state in micelles with an aggregate number n= 2 as suggested earlier by Giles et al. [31]. This brings the area value (17.5 m^2/g) to within the estimated nitrogen surface area (16 m^2/g), which means a more complete coverage of the charred surface with a mono-

layer of aggregated dye molecules [33].

4. Conclusion

Scanning electron microscopy studies and analysis of the N_2/77 K adsorption-desorption isotherms revealed that the surface morphology and porous structure depends strongly on the sample mode of activation. The adsorptive behavior of these ACs towards MB revealed the following: i) The Langmuir and Freundlich adsorption isotherm models are applicable,but application of the Langmuir model gives a better fit, ii) The dye adsorption capacity increases with the increase of the impregnate concentration, iii) The H_3PO_4-ACs heat treated in steam / N_2 atmosphere exhibit more higher affinity towards MB adsorption compared to those obtained under the same conditions but in N_2 atmosphere, iv) The H_3PO_4-ACs are characterized by very high efficiency to adsorb MB compared to the KOH-activated carbon prepared under the same conditions, v)The relatively high adsorption of MB by the steam AC, vi) A large increase in MB adsorption capacity with raising the burn-off value.

References

[1] O. Ioannidou , A. Zabaniotou ; Renew. Sust. Energ. Rev.11 (2007)1966.

[2] K. Wilson, H. Yang, W. S.Chung , E. M.Wayne, Bioresource Technol. 97 (2006) 2266.

[3] M. Sadiq , S. Hessian; Modern Res. in Catal. 2(2013) 148.

[4] X. Lu, M. Jaroniec , R. Madey, Langmuir **7** (1991) 173.

[5] M. Manoochehri**,** A. Khorsand , E. Hashemi**,** *Carbon Lett. 13(2) (2012) 115.*

[6] B. S. Girgis , A. A. El-Hendawy, Micropor and Mesopor Mater. 52 (2002) 105.

[7] E. Mutegoa, I. Onoka , A. Hilonga, Res.J. in Eng. and Appl. Sci. 3(5) (2014) 327.

[8] N.A. Fathy, B.S. Girgis, L. B. Khalil , J.Y. Farah, Carbon lett. 11(3) (2010) 224.

[9] I. Kula, M. Uğurlu, H. Karaoğlu , A. Çelikc, Biores.Technol.99(3) (2008) 492.doi: 10.1016/j.biortech.2007.01.015. [PubMed] [Cross Ref].

[10] F. Boudrahem, A. Soualah , F. Aissani-Benissad, J Chem Eng Data. 56(5) (2011) 1946.doi: 10.1021/je1009569. [Cross Ref]

[11] B.S. Girgis, A.A. Attia , N.A. Fathy, Coll. Surfaces. 299A (2007) 79.

[12] R.C. Bansal, J.B. Donnet , H.F. Stoeckli, Active Carbon, Marcel Dekker, New York, 1988.

[13] J. Gao, Y. Qin, T. Zhou, D. Cao, P. Xu, D. Hochstetter , Y. Wang, J. Zhejiang Univ. Sci. B., 14(7)(2013) 650. doi: 10.1631/jzus.B12a0225 .[PMCID] [Cross Ref]

[14] Y. Feng, M. La, S. Li, F. Yang, www.witpress.com. doi:10.2495/ICBEEE130801. 2014[Cross Ref]

[15] J. W. Hassler, Activated Carbon, Chemical Publishing Co. Inc, New York, 1963.

[16] K. Kadirvelu, M. Kavipriya, C. Karthika, M. Radhika, N. Vennilamani ,S. Pattabhi; Bioresour Technol. 87(2003) 129.

[17] M. Ahmedna, W.E. Marshall , R.M. Rao, Bioresour Technol. 71(2000) 113.

[18] A. Aygun, S. Yenisoy-Karakas , I. Duman; Micropor Mesopor Mater. 66(2003) 189.

[19] B.S. Girgis, S.S. Yunis , A.M. Soliman, Mater. Lett. 57(2002) 164.

[20] X.U. Tao , L.I.U Xiaoqin. , Chinese J of Chem. Eng.16(3) (2008) 401.

[21] J.X. Zhang , L.L. Ou; Water Sci. Technol. 67(4) (2013) 737.doi: 10.2166/wst.2012.605. [Cross Ref]

[22] W.Heschel , E. Klose, Fuel, 74 (1995)1786.

[23] M. M. Girgis, J Mater Sci. 28 (1993) 4925.

[24] S. Brunauer, P. H. Emmett , E. Teller, J Am Chem Soc. 60 (1938) 309.

[25] K. S. W. Sing, Surface Area Determination, (D. H. Everett and R. H. Ottewill, Ed.), Butterworths, London, p. 25, 1970.

[26] M. I. Badawy , H. AbouWaly; Bull. NRC, Egypt.20 (1995) 429.

[27] S. Brunauer, L. S. Deming, W. S. Deming , E. J. Teller, J Am Chem Soc.62(1940)1723.

[28] S.J.Gregg , K. S. W. Sing: Adsorption, Surface Area and Porosity, 2nd Ed. Academic Press, New York, 1982.
[29] M. J. Sellez – Perez , J. M. Martin – Martinez, Fuel. 70 (1991) 877.
[30] C. H. Giles, T. H. MacEwan, S. N. Nakhwa , D. Smith, J Chem Soc.3973(1960).
[31] C. H. Giles, A. P. D. D'Silva, A. S. Trivedi, in Proceedings of the International Symposium on Surface Area Determination, Bristol (1969).Butterworths, 317 (1970).
[32] C. H. Giles, J Am Chem Soc. 91(1969)759.
[33] B. S. Girgis, L. B. Khalil , T. A. M. Tawfik, J. Porous Mater. 9(2002) 105.